Lancaster, David George; Gross, S.; Ebendorff-Heidepriem, Heike; Kuan, K.; Monro, Tanya Mary; Ams, M.; Fuerbach, A.; Withford, M. J.

Fifty percent internal slope efficiency femtosecond direct-written Tm3+:ZBLAN waveguide laser, *Optics Letters*, 2011; 36(9):1587-1589.

Fifty percent internal slope efficiency femtosecond direct-written Tm^{3+}:ZBLAN waveguide laser

**D. G. Lancaster,[1,*] S. Gross,[2] H. Ebendorff-Heidepriem,[1] K. Kuan,[1] T. M. Monro,[1]
M. Ams,[2] A. Fuerbach,[2] and M. J. Withford[2]**

[1]*Institute for Photonics and Advanced Sensing, School of Chemistry & Physics, University of Adelaide, Adelaide, South Australia, 5005, Australia*

[2]*Centre for Ultrahigh bandwidth Devices for Optical Systems, MQ Photonics Research Centre, Department of Physics and Astronomy, Macquarie University, North Ryde, New South Wales 2109, Australia*

**Corresponding author: david.lancaster@adelaide.edu.au*

Received February 18, 2011; revised March 24, 2011; accepted March 25, 2011;
posted March 30, 2011 (Doc. ID 142923); published April 22, 2011

We report a 790 nm pumped, Tm^{3+} doped ZBLAN glass buried waveguide laser that produces 47 mW at 1880 nm, with a 50% internal slope efficiency and an M^2 of 1.7. The waveguide cladding is defined by two overlapping rings created by femtosecond direct-writing of the glass, which results in the formation of a tubular depressed-index-cladding structure, and the laser resonator is defined by external dielectric mirrors. This is, to the best of our knowledge, the most efficient laser created in a glass host via femtosecond waveguide writing. © 2011 Optical Society of America

OCIS codes: 140.0140, 130.2755.

Direct writing of waveguides (WGs) in crystals and glasses is an emerging technology that enables the rapid fabrication of WG lasers in a range of rare-earth doped hosts. The advantages of these directly written WGs over other WG fabrication techniques are the single-step optical processing and consequent geometrical flexibility. The ultrafast direct-write process uses focused femtosecond (fs) laser pulses to induce a permanent refractive index change in dielectric media [1]. WGs written into bulk laser materials improve laser performance over unguided lasers due to the intrinsic pump and laser mode overlap. The tailored WG modes can give diffraction limited beam quality and allow convenient pigtailing to fibre optics.

Heavy-metal fluoride glass is well known for its high IR transparency, especially in its most common composition, ZBLAN (ZrF_4-BaF_2-LaF_3-AlF_3-NaF), thereby making it an attractive host for mid-IR emitting rare-earth ions [2]. A previous study on ultrafast direct writing in ZBLAN glass fibers with a focused low repetition rate (RR) and high pulse energy fs laser demonstrated fiber Bragg gratings based on reduced refractive index regions of $\Delta n = -1 \times 10^{-3}$ [3]. Other work using high pulse energies demonstrated the writing of damage lines that guided light with increased refractive index [4] and self-channelled plasma filament WGs [5]. Our initial direct-write investigations of ZBLAN, using both low RR/high pulse energy and high RR/low pulse energy fs lasers, resulted in regions of reduced refractive index, consistent with [3]. This confirmed that a depressed-index-cladding geometry is required to demonstrate light guidance and lasing in ZBLAN for our direct-write regime.

The most efficient directly written WG laser in a glass host reported to date is a 1.5 μm Er^{3+}, Yb^{3+} codoped phosphate glass laser achieving a 21% slope efficiency and power of 50 mW [6]. In YAG, fs laser irradiation has been shown to induce defects, enabling a depressed cladding structure to be written, and the first Nd^{3+} laser reported achieved 170 mW with an 11% internal efficiency [7]. A 75% slope efficiency and 0.8 W power was recently reported in a stress-induced Yb:YAG WG [8].

The first reported direct-written 2 μm Tm^{3+} doped WG laser was in a germanate glass host with a direct-write WG channel possessing a positive index change and demonstrating an incident slope efficiency of <2% [9].

We report what we believe to be the most efficient (50% slope efficiency) direct-write depressed cladding WG laser in a glass host. This is also the first report of a direct-write ZBLAN glass WG laser.

The WGs were fabricated with a commercial ultrafast Ti:sapphire oscillator (FEMTOSOURCE XL 500—Femtolasers GmbH, 800 nm center wavelength, 5.1 MHz RR, 550 nJ pulse energy, 50 fs pulse duration), which was focused into the bulk sample using a 1.25 NA 100× oil immersion objective, while the sample was translated using a set of computer controlled XYZ air-bearing translation stages. The combination of high NA focusing and high RR causes cumulative heating followed by heat diffusion [10]. This results in structures of quasi-circular cross section with diameters of up to 50 μm. The deposited heat causes a change in the glass structure associated with a relative drop in n of $\sim 1.5 \times 10^{-3}$.

The ZBLAN glass is doped with 2.0 mol. % TmF_3, (3.72×10^{26} ions/m^3 of Tm^{3+}) to allow efficient two for one cross relaxation of the Tm^{3+} ion when pumped at 790 nm. The ZBLAN samples were fabricated in a controlled atmosphere glass melting facility using 50 g batch sizes [11]. For this work the WG substrates were diced using a CNC diamond saw into chips measuring 9 mm long, 8 mm wide, and 2 mm high. The top face of each sample was polished to optical grade, thereby allowing the ultrafast direct-write laser to be focussed through this surface. Each chip was inscribed by the fs laser with up to 42 WGs at a depth of 150 μm. After WG writing, the end faces were polished back by ~250 μm to reveal the WG ends.

Microscope images of the end views of three WG geometries are shown in Fig. 1. These structures approximate the well-known W WG geometry (see inset

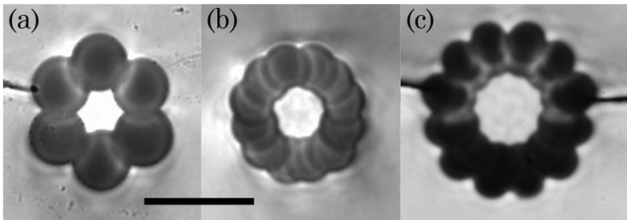

Fig. 1. (a)–(c) Range of waveguide structures fs laser written in ZBLAN glass. Structures with increasing complexity were produced to explore waveguide losses as a function of cladding structure and thickness. The writing laser beam entered from the top of the images. Scale bar corresponds to 50 μm.

of Fig. 3) [12], which can support guided modes provided that the depressed region of the cladding is sufficiently wide for the given index contrast. Structures with increasing complexity [Figs. 1(a)–1(c)] were written with the aim of achieving a more uniform reduced refractive index in the cladding layer and increased cladding diameters. Note that while all structures guided light, only the structure in Fig. 1(c) achieved lasing (this is consistent with the numerical modeling predictions below).

The WG in Fig. 1(a) is composed of six cylinders arranged in a hexagon around the unexposed core and written using 60 nJ pulses; Fig. 1(b) is composed of 12 overlapped cylinders (65 nJ), while Fig. 1(c) is 24 cylinders formed from two partially overlapping rings of 12 cylinders each (50 nJ pulses) with a core diameter of ~30 μm. The depressed claddings for all WGs were written sequentially from the bottom to the top to avoid focusing through previously modified glass, while the sample was moved at 1000 mm/ min. The stress fracture apparent in Figs. 1(a) and 1(c) does not appear to affect the guiding behavior, and we attribute it to the high density of the devices, which have a separation of just 150 μm.

To explore the effect of writing depressed cylinders in close proximity to each other (e.g., two overlapping rings), high resolution refractive index profiles were taken at 637 nm with a refractive index profilometer (RINCK Elektronik). The main image in Fig. 2 shows the absolute refractive index profile of a 24-cylinder WG structure fabricated at 50 nJ, with the inset showing an optical microscope image of the same WG. The n data reveals a net Δn change in the ring structures of $\sim -1 \times 10^{-3}$ to -1.5×10^{-3}, as well as localized regions with slightly increased n, possibly due to stress. Further studies will be necessary to map the Δn as a function of pulse energy and cylinder overlap, as well as optimizing the placement of the direct-write cylinders to reduce confinement losses.

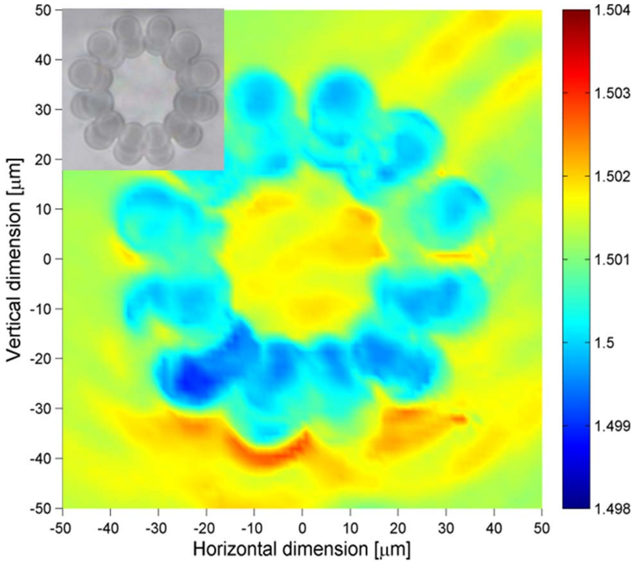

Fig. 2. (Color online) Absolute refractive index profile at 637 nm of the WG formed from 24 partially overlapping cylinders direct written at 1 m/ min. Inset shows corresponding optical microscope image.

To understand the guiding behavior of these WGs, we investigated the confinement loss of idealized W WGs as a function of cladding diameter and index contrast. In general W type WGs support "leaky" modes in which the imaginary propagation constant is associated with the confinement loss of the guided mode.

Numerical modelling results, using the exact electromagnetic solution to a circularly symmetric W refractive index profile, are shown in Fig. 3 for two representative cladding Δn's of -1×10^{-3} and -1.5×10^{-3} and a core diameter of 30 μm. As shown in Fig. 3, the fundamental mode (FM) confinement losses at $\lambda = 1.89$ μm decrease strongly with increasing Δn contrast and cladding width, with the first higher order mode having a substantially higher loss (~25 × FM loss) for a cladding width of 23 μm, which is the approximate cladding width of the structure in Fig. 1(c), thus enabling such structures to be "effectively single mode." At a cladding width of 23 μm, the predicted FM losses are sensitive to Δn and are 0.018 dB/cm (0.7% per round trip) for $\Delta n = -1.5 \times 10^{-3}$, increasing to 0.14 dB/cm (5.6% per round trip) for $\Delta n = -1 \times 10^{-3}$.

On modelling the WG shown in Fig. 1(b), FM losses are substantially higher at 1 to 3.5 dB/cm for Δn's of -1.5×10^{-3} to -1×10^{-3}, respectively. This corresponds to predicted roundtrip cavity losses of 34% (for $\Delta n = -1.5 \times 10^{-3}$) to 77% (for $\Delta n = -1 \times 10^{-3}$), which would explain the nonlasing observed from the WG shown in Fig. 1(b). We attribute the nonlasing of the WG shown in Fig. 1(a) to the partially overlapped cylinders leading

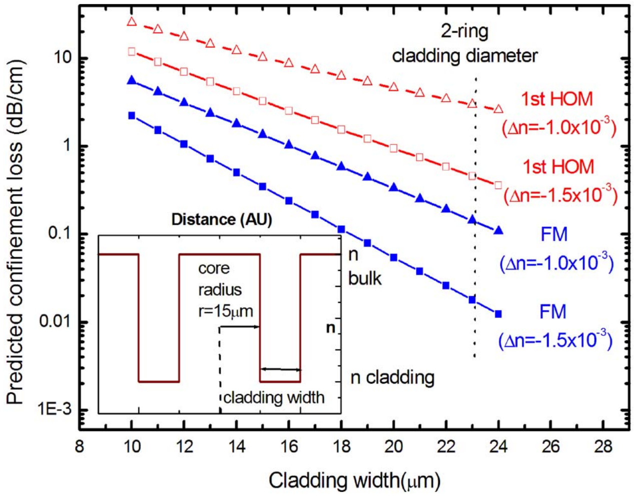

Fig. 3. (Color online) Predicted confinement loss at $\lambda = 1.9$ μm for a W depressed cladding WG. Loss of the FM and first higher order mode as a function of cladding width.

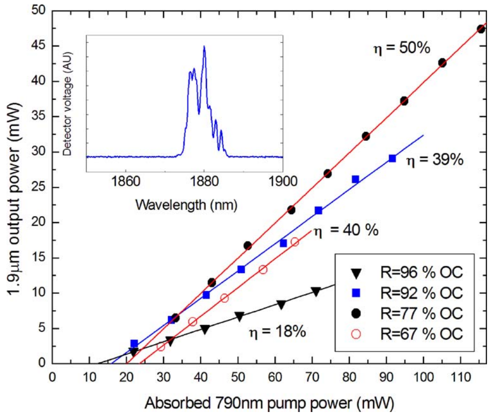

Fig. 4. (Color online) Measured internal slope efficiencies as a function of absorbed 790 nm pump power for the Tm^{3+}:ZBLAN WG laser. The inset is the measured Tm^{3+} waveguide laser spectrum.

to regions of narrow cladding, and a low average Δn. If we assume $\Delta n = -1 \times 10^{-3}$ and a cladding width of $15\,\mu$m, the predicted loss is 11 dB/cm, indicating that laser operation of this WG is not feasible. (While the W model is clearly an approximation of the geometry of this WG, it provides useful insight into the conditions required for lasing to occur.)

To pump the 9 mm long, $30\,\mu$m diameter Tm^{3+} doped WG shown in Fig. 1(c), 150 mW of 790 nm diode laser light was delivered by a $25\,\mu$m diameter, 0.10 NA fiber. This was free-space imaged into the WG using a pair of $f = 20$ mm aspheric lenses. The laser resonator was formed using external dielectric coated mirrors that were butted up to the uncoated WG ends. The input mirror was highly reflecting at $1.9\,\mu$m and highly transmitting at 790 nm. The $1.9\,\mu$m output couplers (OCs) available ranged from 4% to 33%, and the 790 nm reflection for each OC was measured. To remove residual pump light after the WG, an uncoated Si window was used ($T = 53\%$ at 1880 nm).

The measured slope efficiencies as a function of absorbed power for a range of output couplers are shown in Fig. 4 ($\alpha_{\mathrm{Tm}^{3+}:\mathrm{ZBLAN},\,\lambda=790\,\mathrm{nm}} = 5.1$ dB/cm). The best result was achieved using the $30\,\mu$m diameter WG and an $R = 77\%$ OC. This gave a 50% internal slope efficiency, 21 mW threshold, and 47 mW of output. The free running laser spectrum was measured to be centered at $\lambda = 1880$ nm with a broad 5 nm bandwidth (Fig. 4 inset).

To estimate the WG propagation loss, we performed a Findlay–Clay analysis on the lasing data plotted in Fig. 4, which gave an estimated loss of 0.22 ± 0.06 dB/cm. This value should be considered an upper limit, since it includes ground state absorption losses due to the three-level nature of the $1.9\,\mu$m transition in thulium.

The beam quality was measured by determining the focused beam widths on an array sensor (Spiricon Pyrocam) and was measured to be $M^2 = 1.7 \pm 0.2$. A Gaussian beam profile in the far field was observed that would be expected for the fundamental mode. The non-diffraction-limited beam quality we attribute to nonuniformities in the cladding Δn and the noncircular waveguide geometry. The beam quality will be further investigated in future work.

We expect the efficiency to improve by fabrication of appropriate dielectric coatings on the slab and by optimizing device length, WG confinement, and dopant concentration. This result indicates that ZBLAN is a promising host glass for efficient depressed cladding WG lasers, and its midinfrared transparency and low phonon energy should allow access to longer wavelength laser transitions.

In conclusion, we have demonstrated a 790 nm pumped thulium $1.9\,\mu$m WG laser that has a 50% internal slope efficiency, M^2 of 1.7 ± 0.2 and pump-power-limited output of 48 mW. To our knowledge, this depressed cladding WG laser is the most efficient fs direct-write glass WG laser reported to date, has achieved the highest power at $\lambda > 1.6\,\mu$m, and is the first ZBLAN direct-write WG laser.

This work was produced with the assistance of the Australian Research Council (ARC) under the Centres of Excellence and Linkage Infrastructure, Equipment and Facilities programs, as well as the South Australian Premier's Science and Research Fund. The authors acknowledge S. Warren Smith for the MATLAB code for the exact EM solution for the WG W model and A. Dowling for technical support. T. Monro acknowledges the support of an ARC Federation Fellowship.

References

1. K. M. Davis, K. Miura, N. Sugimoto, and K. Hirao, Opt. Lett. **21**, 1729 (1996).
2. X. Zhu and N. Peyghambarian, Adv. OptoElectron. **2010**, 501956 (2010).
3. M. Bernier, D. Faucher, R. Vallee, A. Saliminia, G. Androz, Y. Sheng, and S. L. Chin, Opt. Lett. **32**, 454 (2007).
4. K. Miura, J. Qiu, T. Mitsuyu, and K. Hirao, J. Non-Cryst. Solids **256–257**, 212 (1999).
5. S. H. Cho, W. S. Chang, J. G. Kim, and K. H. Whang, Appl. Phys. Lett. **91**, 121907 (2007).
6. G. Della Valle, S. Taccheo, R. Osellame, A. Festa, G. Cerullo, and P. Laporta, Opt. Express **15**, 3190 (2007).
7. A. G. Okhrimchuk, A. V. Shestakov, K. Khrushchev, and J. Mitchell, Opt. Lett. **30**, 2248 (2005).
8. J. Siebenmorgen, T. Calmano, K. Petermann, and G. Huber, Opt. Express **18**, 16035 (2010).
9. R. R. Thomson, G. Jose, F. Bain, A. A. Lagatsky, N. D. Psaila, A. K. Kar, A. Hja, W. Sibbett, and C. T. A. Brown, in *Conference on Lasers and Electro-Optics/Quantum Electronics and Laser Science Conference* (Optical Society of America, 2010), paper CtuU5.
10. C. B. Schaffer, J. F. Garcia, and E. Mazur, Appl. Phys. A **76**, 351 (2003).
11. H. Ebendorff-Heidepriem, T. C. Foo, R. C. Moore, W. Zhang, Y. Li, T. M. Monro, A. Hemming, and D. G. Lancaster, Opt. Lett. **33**, 2861 (2008).
12. J. Hu and C. R. Menyuk, Adv. Opt. Photon. **1**, 58 (2009).